JCES

Journal of Civil Engineering and Structures

Vol.1 , Issue.1 , September 2017

ISSN (Online): 2588-3275

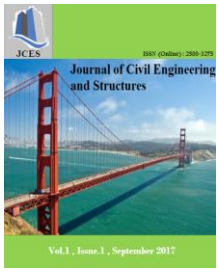


# Investigation of influence the pressure and stress on the water in buried concrete pipes in the different soil under blast loading

**Mojtaba Hosseini[1], Peyman Beiranvand[2*], Leila Kalantari[3]**

[1] Associate Professor, Department of Civil Engineering, Lorestan University, Khorram abad, Iran;
[2*] PhD Candidate, Department of Civil Engineering, Razi University, Kermanshah, Iran;
[3] MSc, Department of Civil Engineering, Doroud Branch, Islamic Azad University, Iran;
[*] Correspondence: peyman51471366@gmail.com; Tel.: +98-937-865-1620

Received: 13 June 2017 ; Revised: 13 August 2017 ; Accepted: 5 September 2017; Published: 7 September 2017

**Abstract:** Soil mantle is an effective factor in decreasing damege against explosion so, by increasing the density of the soil, the pressure and the stress on the buried pipe increased. In this research, a parametric study on the buried pipe in the soil and due to blast loading have been performed. Effect of various parameters such as physical properties of water, air, soil, concrete pipe and T.N.T have been investigated. The arbitrary Lagrangian-Eulerian (ALE) method has been used by the LS-DYNA software. The pressure on the pipe and the stress in the important point of the pipe have been obtained. The results show that, In general soil with the more density has more pressure and strees transfers on the pipe and if the density of soil is low, the damege to the pipe when the explosion occure is low and acts as a damper under waves of explosion.

**Keywords:** Explosion, Buried pipe, Lagrangian-Eulerian, Stress, Pressure.

## 1. Introduction

To study the effect of blast loads on the buried structures, in added to the experimental and semi-experimental methods, the numerical methods also can be used. The blast simulation has been performed in three stages: (1) explosion formation and generation the crater, (2) propagation of the blast waves, (3) calculation of the response of the structures. The numerical methods can be devided in three categories: cascaded method, incompletely compound method and completely compound method. Young and Hinman used the cascaded method to analyse the buried pipes [1,2].In this method the field stress on the pipe due to calcuted and then these stresses applied to the pipe as boundary condition. In the cascaded methods, the interaction between soil and pipe has been ignored. Althoug the method is simple but their results maight be unreal. Zimerman combined the stage 1 ans 2 above, and reduced the simulation to two stage [3].He modeled the soil by the finited difference method, The structure by the finite element method, and considered the blast loading as pressure time history.He concluded that this method is unsuitable for unsymmetric structure and lie in the low depth. The completely compound, use by Wang and Lu [4].In this method all the three stage have been considered simultanously. They modeled the soil near the explosion by the smothed-particle-hydrodynamics (SPH) method, and the soil far from the explosion by the finite element method. Yao studied the buried pipe subjected to the blast loading , but in their investigation, there is no fluid in the pipe [5].Yan and Xu simulated the peak over pressure of the blast on the air [6].Anirban studied the effect of surface blast on the dry and cohesion less soil. He used the ALE method and concluded



DOI: 10.21859/jces-01015

that the important parameter that influence that analyse is the metal behavior of soil in the large deformation.for calculating the blast load on the structure the codes TM5-1300 and TM5-885 can be use to calculate the blast loading on the structures [7].

*1.1 Explosion parameters*

Add characteristics parameters such as pressure, usually with the arrival of shock waves, adding pressure on the blast, blast wave transit time are determined. This parameter is a function of the strength of explosives, explosion point to the measured distance and angle can be calculated analytically or experimentally.

*1.2 Scaling laws*

One of the most critical parameters for blast loading computations is the distance of the detonation point from the structure of interest. The peak pressure value and velocity of the blast wave, which were described earlier, decrease rapidly by increasing the distance between the blast source and the target surface, as shown in Figure 2. In the figure only the positive phases of the blast waves are depicted, whose durations are longer whenever the distance from the detonation point increases.

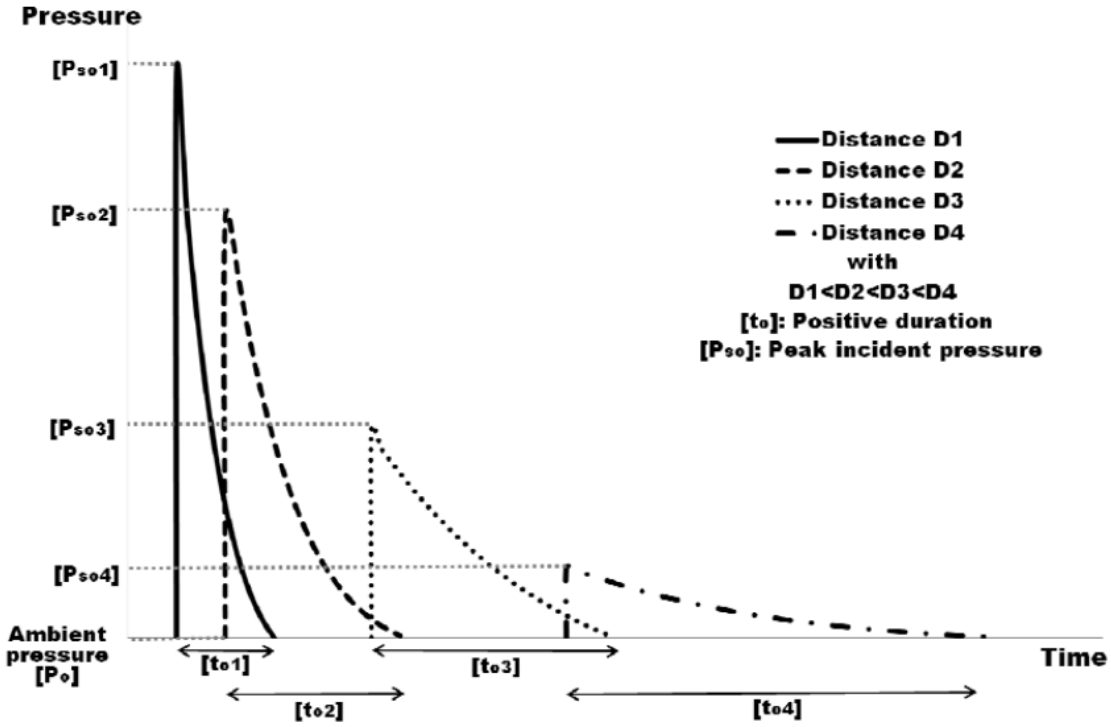


**Figure 1.** Influence of distance on the blast positive pressure phase [8]

The effect of distance on the blast characteristics can be taken into account by the introduction of scaling laws. These laws have the ability to scale parameters, which were defined through experiments, in order to be used for varying values of distance and charge energy release. The experimental results are, in this way, generalized to include cases that are different from the initial experimental setup. The most common blast scaling laws are the ones introduced by Hopkinson-Cranz and Sachs. The idea behind both

formulations is that during the detonation of two charges of the same explosive that have similar geometry but different weight and are situated at the same scaled distance from a target surface, similar blast waves are produced at the point of interest as long as they are under the same atmospheric conditions. Sachs scaling is also suitable in the case of different atmospheric conditions. According to Hopkinson-Cranz law, a dimensional scaled distance is introduced as described by Equation (1),

$$Z = \frac{R}{\sqrt[3]{W}} \quad (1)$$

where, R is the distance from the detonation source to the point of interest [m] and W is the weight (more precisely: the mass) of the explosive [kg].Thus, suppose that an explosive charge of weight $W_1$ and characteristic size $d_1$, situated at distance $R_1$ from the point of interest, produces at this point a blast wave of peak overpressure P, impulse $i_1$, duration $t_{o1}$, with arrival time $t_{a1}$ and that $\lambda = R_1/\sqrt[3]{W_1}$.Then, what this scaling law implies is that a blast wave with the same peak overpressure P and similar form would be produced at this point by another explosive charge $W_2$ of characteristic dimension $d_2 = \lambda d_1$ situated at distance $R_2 = \lambda R_1$. Further, at the given point due to $W_2$ we would have: impulse $i_2 = \lambda i_1$, duration $t_{o2} = \lambda t_{o1}$, and arrival time $t_{a2} = \lambda t_{a1}$.It is essential to underline that under this formulation all distance and time parameters of a blast wave are scaled by the same factor **λ** but pressure and velocity values remain unchanged at similarly analogous times.

*1.3 Loding blast*

Figure 2 shows a typical blast pressure profile. The pressure time-history is divided into a positive and a negative phase. In the positive phase, maximum overpressure, $P_s^+$, is developed instantaneously and decays to atmospheric pressure, $P_0$, in the time $T^+$. For the negative phase, the maximum negative pressure, $P_s^-$, has much lower amplitude than the positive overpressure. The duration of the negative phase, $T^-$, is longer compared to the positive duration. The positive phase is more relevant in studies of blast effects on structures because of its high amplitude of the overpressure and bigger area under the positive phase of the pressure–time curve. Then simplified by a linearly decaying pressure-time history represent the triangular load pattern shown in Figure 3.

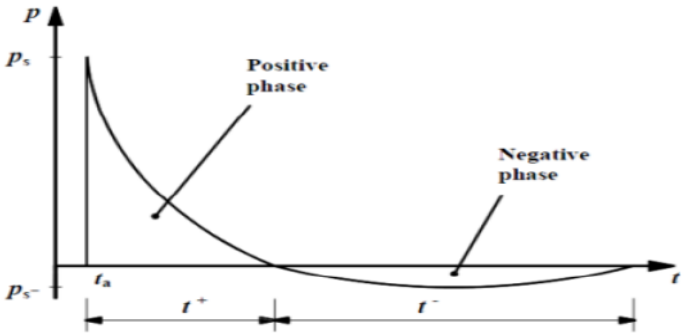


**Figure 2.** characteristics of blast wave [9]

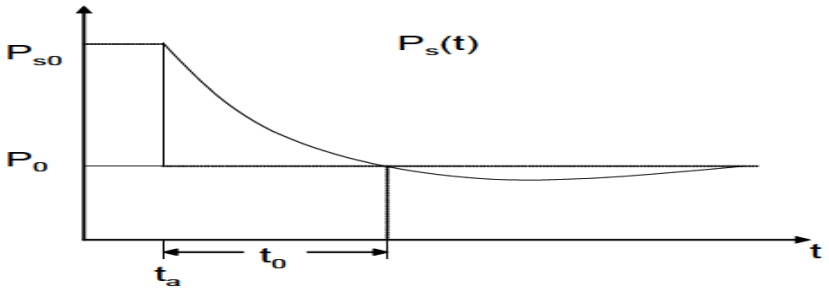


**Figure 3.** A general pressure profile of blast wave [9]

P(t) is the overpressure at time t, $P_{max}$ and $P_s^+$ are maximum over pressure in triangular and exponential loading pattern respectively. Air blast loading can be qualified based on the charge weight and stand-off distance [9]. The duration of explosion pressure on underground structures can be obtained from the following equation:

$$t_d = 2\frac{i_o}{p_o} \quad (2)$$

$$i_o = \rho C x \quad (3)$$

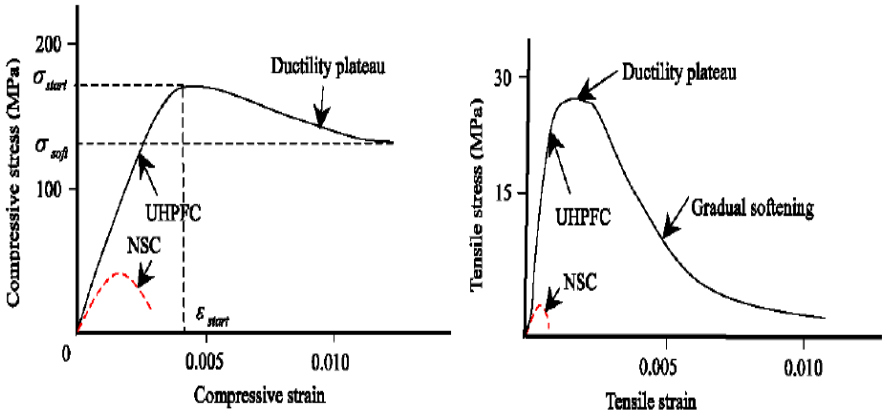


**Figure 4.** Mechanical properties of concrete under compressive load (left) and tensile load (right) [12]

## 2. Numerical Model

The researched pipeline has a circular cross-section, with 0.36 m in inner diameter and 0.4 m in outer diameter. For many previous studies on pipeline loaded explosively, equivalent time-history pressures were used to simulate the loads. Time-history pressures generated with high explosives tend to exhibit large variations, even with identical charges. Obviously, whether the responses of the structure can be predicted strongly depend on the ability to generate "accurate" load functions.In this article, the explosive was modeled explicitly using LS-DYNA material specifically designed for simulating a high explosive detonation. LS-DYNA is a general-purpose finite element program capable of simulating complex real world problems. It is used by the automobile, aerospace, construction, military, manufacturing, and bioengineering industries. LS-DYNA is fully QA'd by LSTC. The code's origins lie in highly nonlinear, transient dynamic finite element analysis using explicit time integration [10,11]. It is assumed that the

explosion will take place at the most unfavorable positions such as the interface of air and soil, above the pipeline. For the sake of saving computation time, a 1/4 symmetrical geometrical model with a size of 0.6 m×1.8m×2m was established (Figure 5-b), In the finite element model (Figure 5-a). the eight-node element of SOLID 164 was adopted for the 3D explicit analysis. In order to prevent the element distortion in large deformation and nonlinear structural analyses, an arbitrary Lagrangian-Eularian (ALE) algorism was used in this paper. The TNT charge, the air, the soil and the liquid in a pipeline were modeled with ALE multi-material meshes, but the pipeline with Lagrangian meshes, while the minimal time step was controlled by the smallest element size in the explicit integral method, and the globe uniform mesh size was set to be 5 cm.Furthermore, the transitional displacement of the nodes normal to the symmetry planes was constrained. Non-reflecting boundary condition was applied to the other two lateral surfaces and the bottom surface, and the free boundary condition is used for the upper surface. Five kinds of materials were involved in this finite element model: air, TNT charge, pipeline, water and soil.

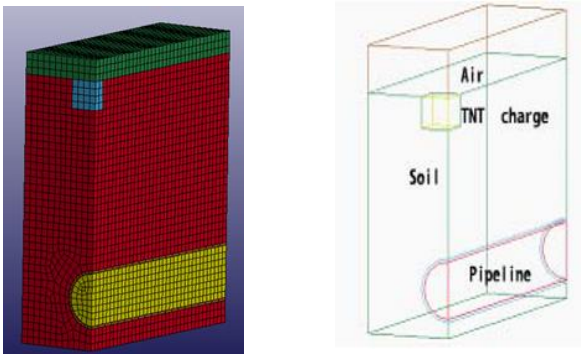


( a) (b)

**Figure 5. (**a) finite element model, (b) geometric model

*2.1 Model of explosives*

In this paper, The TNT charge was modeled by the high explosive material model and the Jones-Wilkins-Lee (JWL) equation of state. The JWL equation of state defined the pressure by the following equation:

(4)

$$P = A\left[1-\frac{\omega}{R_1 V}\right]e^{-RV_1} + B\left[1-\frac{\omega}{R_2 V}\right]e^{-R_2 V} + \frac{\omega E}{V}$$

Where P is the pressure, Where A,B, $R_1$, $R_2$,ω were the equation coefficients, and V was the initial relative volume and E was the initial relative volume. Table (1) gives the parameters used in the TNT charge model:

**Table 1.** Parameters of the TNT charge

| Numerical Values | Material Properties |
|---|---|
| 1.63E+03 | ϱ |
| 6.93E+03 | $V_D$ |
| 2.10E+01 | $P_{CJ}$ (Gpa) |
| 3.74E+02 | A (Gpa) |
| 3.23E+00 | B (Gpa) |
| 4.15E+00 | $R_1$ |
| 9.50E-01 | $R_2$ |
| 3.80E-01 | ω |
| 1.00E+00 | V |
| 6.00E+09 | $E_0$ |

*2.2 Model of Air*

Air material model was commonly modeled by null material model with a linear polynomial equation of state (EOS), which defined the pressure by the following equation:

(5)

$$P = C_0 + C_1\mu + C_2\mu^2 + C_3\mu^3 + \left(C_4 + C_5\mu + C_6\mu^2\right)E_0$$

Where the parameter P is the pressure, $\mu$ is defined as $\frac{\rho}{\rho_\circ} - 1$, $\rho$ is the density and $\rho_\circ$ was the reference density. $C_0$ To $C_6$ were the equation of constant coefficients. the parameter $E_0$ is the initial internal energy of reference specific volume per unit. table (2) gives the parameters used in the air model:

**Table 2.** parameters of the air

| Numerical Values | Material Properties |
|---|---|
| 1.29 | ϱ |
| 0 | $C_0$ |
| 0 | $C_1$ |
| 0 | $C_2$ |
| 0 | $C_3$ |
| 0.4 | $C_4$ |
| 0.4 | $C_5$ |
| 0.4 | $C_6$ |
| $2.5\times10^5$ | $E_0$ |
| 1 | $\varrho_0$ |

*2.3 Model of concrete Pipe*

the model used in this article to simulate concrete target is the Johnson Holmquist model (Holmquist et al., 1993; Johnson 1998).compressive strength of concrete pipes ConA, ConB and ConC are 48, 51and 156 Mpa.Table 3 to 5 gave the parameters used in the pipeline model:

**Table 3.** parameters of the concrete A[12]

| Numerical Properties | Material Properties | Numerical Values | Material Properties |
|---|---|---|---|
| 2440 | $R_O$ | 0.00058 | $U_C$ |
| 1.36E+10 | G | 1.0536E+6 | $P_L$ |
| 0.75 | A | 0.1 | $U_L$ |
| 1.95 | B | 0.03 | $D_1$ |
| 0.007 | C | 1 | $D_2$ |
| 0.76 | N | 1.74E+10 | $K_1$ |
| 4.80E+7 | $F_C$ | 3.88E+10 | $K_2$ |
| 4E+6 | T | 2.98E+10 | $K_3$ |
| 0.001 | EPSO | 0.3 | Fs |
| 0.01 | $EF_{MIN}$ | 1.36E+7 | $P_C$ |
| 11.7 | $SF_{MAX}$ | | |

**Table 4.** parameters of the concrete B[13]

| Numerical Values | Material Properties | Numerical Values | Material Properties |
|---|---|---|---|
| 2330 | $R_O$ | 0.00058 | $U_C$ |
| 1.36E+10 | G | 1.05E+6 | $P_L$ |
| 0.75 | A | 0.1 | $U_L$ |
| 1.65 | B | 0.03 | $D_1$ |
| 0.007 | C | 1 | $D_2$ |
| 0.76 | N | 1.74E+10 | $K_1$ |
| 5.1 E+7 | $F_C$ | 3.88E+10 | $K_2$ |
| 3.92 E+6 | T | 2.98E+10 | $K_3$ |
| 0.001 | EPSO | 0.3 | Fs |
| 0.01 | $EF_{MIN}$ | 1.36E7 | $P_C$ |
| 11.7 | $SF_{MAX}$ | | |

**Table 5.** parameters of the concrete C[12]

| Numerical Values | Material Properties | Numerical Values | Material Properties |
|---|---|---|---|
| 2250 | $R_O$ | 0.0001 | $U_C$ |
| 3.32E+10 | G | 8.5E+08 | $P_L$ |
| 0.79 | A | 0.1 | $U_L$ |

| | | | |
|---|---|---|---|
| 1.6 | B | 0.05 | $D_1$ |
| 0.007 | C | 1 | $D_2$ |
| 0.61 | N | 8.5E+09 | $K_1$ |
| 1.56 E+08 | $F_C$ | 1.71E+10 | $K_2$ |
| 8.4 E+6 | T | 2.08E+10 | $K_3$ |
| 0.001 | EPSO | 0.3 | Fs |
| 0.01 | $EF_{MIN}$ | 1.9E+7 | $P_C$ |
| 12.5 | $SF_{MAX}$ | | |

G : elastic shear modulus; A : intact normalized strength parameter; B : fractured normalized strength parameter; C : strength parameter (for strain rate dependence); N : intact strength parameter (pressure exponent); EPSO: reference strain rate; T : maximum tensile pressurestrength; $SF_{MAX}$ : maximum normalized fractured strength; $D_1$ : parameter for plastic strain to fracture; $D_2$ : parameter for plastic strain to fracture (exponent);$K_1$ : first pressure coefficient (equivalent to the bulk modulus); $K_2$ : second pressure coefficient; $K_3$ : third pressure coefficient; Fs : failure criteria.

*2.4 Model of Water*

The water was commonly modeled by null material model with a Gruneisen equation of state (EOS), which defines the pressure by the following equation:

(6)

$$P=\frac{\rho_0 C^2\mu\left(1+\left(1-\frac{\gamma_0}{2}\right)\mu-a\frac{\mu^2}{2}\right)}{\left(1-(S_1-1)\mu-S_2\frac{\mu^2}{(1+\mu)}-S_3\frac{\mu^3}{\left((1+\mu^2)\right)^2}\right)}+(\gamma_0+a\mu)\mathrm{E}$$

where the parameter P is the pressure, $\mu$ is defined as $\frac{\rho}{\rho_\circ}-1$, ϱ is density and $\rho_\circ$ is the reference density and $S_1$ to $S_3$ , $\gamma_0$ and a are constant coefficient equation. E is the initial relative volume and C was the sound propagation velocity in the water. table (6) gives the parameters used in the water model:

**Table 6.** parameters of the water

| Numerical Values | Material Properties |
|---|---|
| 1025 | ϱ |
| 1480 | C |
| 142 | $S_1$ |
| 0.33 | $S_2$ |
| 0.7 | $S_3$ |
| 0.5 | $\gamma_0$ |

*2.5 model of soil*

The soil was modeled by a soil and foam model put forward by Krieg in 1972. It was a simple model and operated in some way like a fluid, and had been demonstrated to be useful for soil modeling. The main

parameters in this model: in the first type of soil include: density equal to 1225 kg per cubic meter, Bulk modulus 5.51Mpa, shear modulus 1.72MPa and yield function constants $a_0$=0, $a_1$=0 and $a_2$ =0.87. in the type II of soil in this paper include : density aqual to 1800 kilograms per cubic meter,the shear modulus of 11 Mpa,Bulk modulus of 190 MPa yield function constants $a_0$=0.33MPa2, $a_1$=0.7Mpa and $a_2$=0.33[6].

**3. Elemental determinig of buried concrete pipe under explosion**

In this part, the four elements of H 17668, H 17728, H 17788, and H 17968 according to Figure (6) for analysisin two types of soil with different characteristics under explosion have determined.

Simulation with masses 1.6, 3.2, 4.8, 6.5 and 8 kg were done by ALE method.pressures and stresses changes on concrete pipes with increasing the amount of TNT were presented by some graphs.following Figure (7) show some steps of the model in the software.

**Figure 6.** an element of choice for numerical analysis of concrete pipe

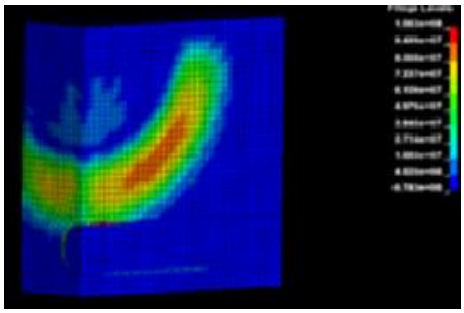

**Figure 7.** analysis of model

**4. Determining the maximum principal stress on selected elements of buried concrete pipe**

In This part, three types of concrete CONA, CONB and CONC in first type of soil were determined and the graphs related to principal stresses in three above concretes were shown in Figure 8 to 11.

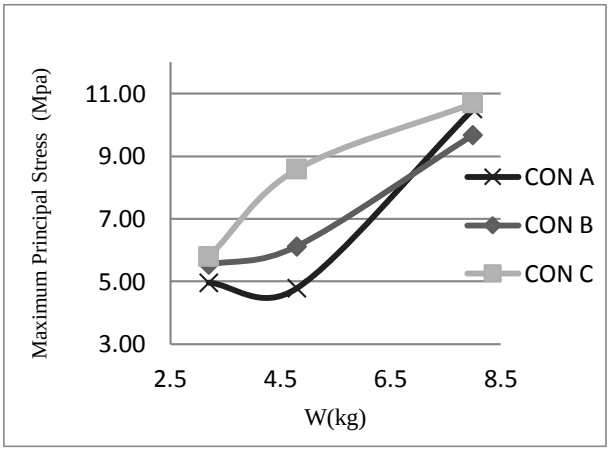


**Figure 8.** Maximum stress values to element H 17968 of soil type I

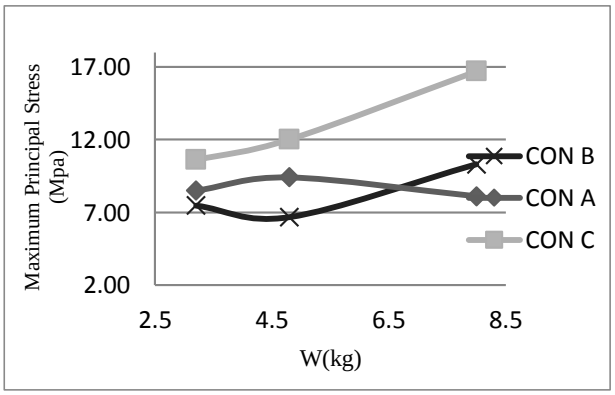


**Figure 9.** Maximum stress values to element H 17788 of soil type I

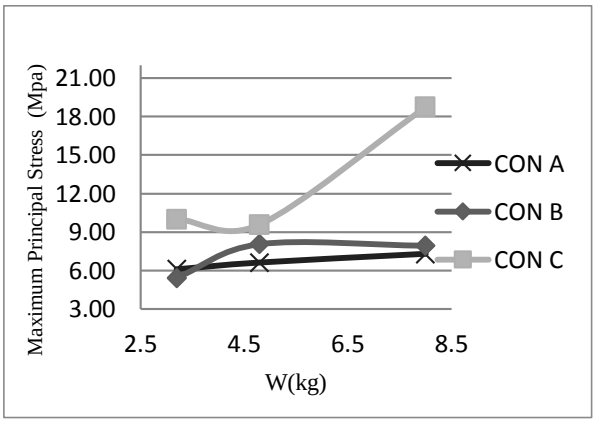


**Figure 10.** Maximum stress values to element H 17728 of soil type I

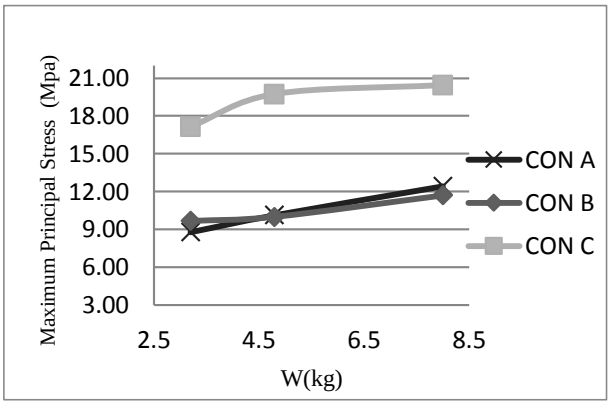


**Figure 11.** Maximum stress values to element H 17668 of soil type I

## 5. The influence of type of soil in publication explosion waves

According to soil mantle is an effective factor in decreasing damege to buried structure against explosion, The results of influence of two types of soil which were used in the masses 3.2, 4.8, 6.5 and 8 kg have presented in 7 to 9 tables:

**Table 7.** the different pressure of the soil type I and II for CON A

| | CON A= 48 MPA | | |
|---|---|---|---|
| different (%) | Pressure Soil 1 (Mpa) | Pressure Soil 2 (Mpa) | Mass (kg) |
| 43.45 | 13.59 | 24.03 | 3.20 |
| 77.21 | 11.95 | 52.43 | 4.80 |
| 77.37 | 13.59 | 60.04 | 6.50 |
| 74.15 | 13.54 | 52.38 | 8.00 |

**Table 8.** the different pressure of the soil type I and II for CON B

| | CON B=51 MPA | | |
|---|---|---|---|
| different (%) | Pressure Soil 1 (Mpa) | Pressure Soil 2 (Mpa) | Mass (kg) |
| 19.19 | 10.99 | 13.6 | 3.20 |
| 75.20 | 13.57 | 54.71 | 4.80 |
| 77.40 | 12.2 | 53.98 | 6.50 |
| 78.54 | 12.86 | 59.92 | 8.00 |

**Table 9.** the different pressure of the soil type I and II for CON C

| | CON C=156 MPA | | |
|---|---|---|---|
| different (%) | Pressure Soil 1 (Mpa) | Pressure Soil 2 (Mpa) | Mass (kg) |
| 83.89 | 20.69 | 128.39 | 3.20 |
| 85.63 | 21.95 | 152.74 | 4.80 |

| | | | |
|---|---|---|---|
| 86.14 | 23.63 | 170.45 | 6.50 |
| 85.61 | 24.27 | 168.61 | 8.00 |

As it is absorved the soil with the more density has more pressure transfers on the pipe and the difference between two types of soil is presented in below tables.In general if the density of soil is low, the damege to the pipe when the explosion occure is low and acts as a damper under waves of explosion.

**6. The operation of buried concrete pipe in soil under explosion globally**

In this part, at first the most stresses applied to the buried concrete pipes in the soil will be determined and in second part most pressure applied to the buried concrete pipes in two types of soil will be determined.the Figure 12 shows the most stress applied to first type of soil and Figure 13 shows the most stress applied to second type of soil for masses 1.6, 3.2,4.8 and 8 kg globally.

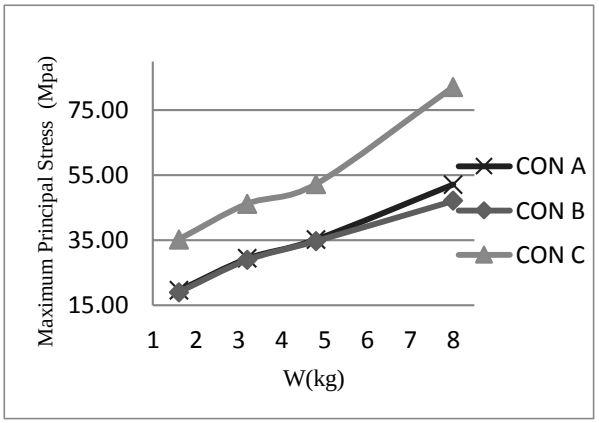


**Figure 12.** The maximum stress applied to the cocrete pipes in soil I of the global

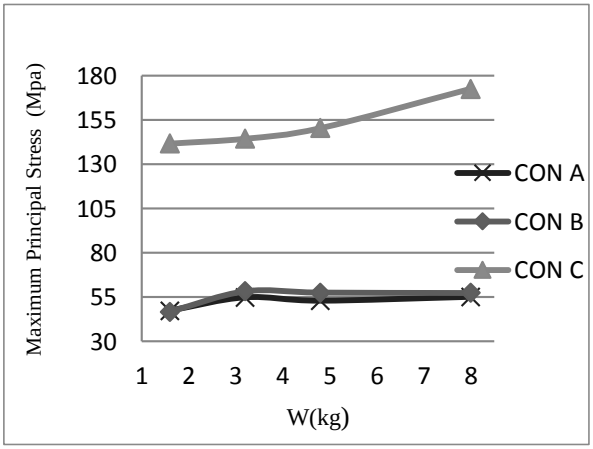


**Figure 13.** The maximum stress applied to the cocrete pipes in soil II of the global

As it is appear in Figure of 12 and 13 ,the maximum stress applied to the concrete pipes with 8 kg mass in first type of soil (CON C) is 82.13 and the maximum stress applied to the concrete pipes with 8 kg mass in second type of soil (CON C) is 172.51 Mpa.

The Figure 14 shows the most pressure applied to the first type of soil and the Figure 15 shows the most pressure applied to the second type of soil for masses 3.2, 4.8, 6.5 and 8 kg globally.

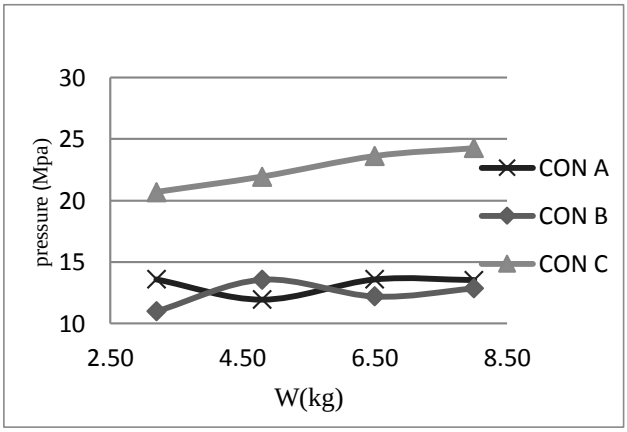


**Figure 14.** The maximum pressure applied to the cocrete pipes in soil I of the global

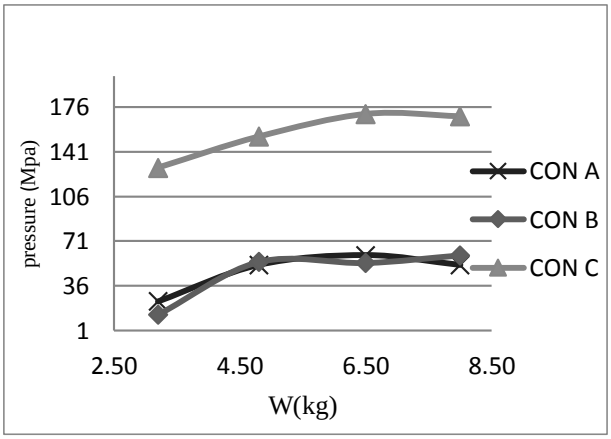


**Figure 15.** The maximum pressure applied to the cocrete pipes in soil II of the global

The maximum pressure applied to the concrete pipes with 8 kg mass in first type of soil (CON C) is 24.27 and the maximum pressure applied to the concrete pipes with 8 kg mass in second type of soil (CON C) is 168.61 Mpa.According to the graphs presented in pressure and stress concrete pipes CON A and CON B and CON C.it is appear that CON C has more compressive resistance rather than CON B and CON A in a constant strain rate, the pressure and stress applied to CON C was more than CON A and CON B.Figure 4 is a verification of the results that mentioned The first part of the article.

**7. Conclusion**

In this paper, two types of soils with different characteristics were studied and the results are as follows:

1. According to soil mantle is an effective factor in decreasing damege to buried structure against explosion so, As it is absorved the soil with

the more density has more pressure and stress transfers on the pipe and if the density of soil is low, the damege to the pipe when the explosion occure is low and acts as a damper under waves of explosion.

2. in the soil I, all of elements (first, second, third and fourth) for CON A under explosion was observed that with the increase of 2.5 times the mass of TNT, the stress level of 1.38 in the first element, the second element 2.12 and the third element 1.19 and fourth element 1.41 times higher.

3. in the soil I, all of elements (first, second, third and fourth) for CON B under explosion was observed that with the increase of 2.5 times the mass of TNT, the stress level of 0.95 in the first element, the second element 1.75 and the third element 1.46 and fourth element 1.21 times higher.

4. in the soil I, all of elements (first, second, third and fourth) for CON C under explosion was observed that with the increase of 2.5 times the mass of TNT, the stress level of 1.57 in the first element, the second element 1.85 and the third element 1.88 and fourth element 1.19 times higher.

5. In global, for CON A under explosion was observed that with an increase of 2.5 times the mass of TNT, for soil I the pressure level is unchange and for the second soil 2.17 times progress.

6. In global, for CON B under explosion was observed that with an increase of 2.5 times the mass of TNT, for soil I the pressure level is 1.17 and for the second soil 4.4 times progress.

7. In global, for CON C under explosion was observed that with an increase of 2.5 times the mass of TNT, for soil I the pressure level is 1.17 and for the second soil 1.31 times progress.

8. In global, for CON A under explosion was observed that with an increase of 5 times the mass of TNT, for soil I the stress level is 2.67 and for the second soil 1.16 times progress.

9. In global, for CON B under explosion was observed that with an increase of 5 times the mass of TNT, for soil I the stress level is 2.49 and for the second soil 1.23 times progress.

10. In global, for CON C under explosion was observed that with an increase of 5 times the mass of TNT, for soil I the stress level is 2.33 and for the second soil 1.22 times progress.

**References**

[1] Yang, Z., (1997), Finite element simulation of response of buried shelters to blast loadings, Finite Elements in Analysis and Design,vol(24) , 113-132.

[2] Hinman, E.E. (1989a), Effect of deformation on the shock response of buried structures subject to explosions, Structures under shock and impact, Elservier, 455-465.

[3] Zimmerman, H., Cooper, G., Carney, J. and Ito, Y. (1990a), Cratering and ground shock environment prediction of buried armor piercing bomb in dry Socorro plaster sand, Technical Report CRT- 3295-010-01, California Research and Technology, Chattsworth Calif.

[4] Wang, Z.Q., Lu, Y., Hao, H. and Chong, K. (2005), A full coupled numerical analysis approach for buried structures subjected to subsurface blast, Comput. Struct., 83(4-5), 339-356.

[5] Yao, A. L. (2009), Numerical simulation of dynamic response of buried pipeline by underground explosion, Journal of Southwest Petroleum University (Science &Technology Edition), 31(4), 168-172.

[6] Yan, S. and Xu, Y. R., Chang, H. Y (2012),Numerical Simulation of Dynamic Response of Buried Pipeline by Ground Explosion., pp. 1159–1166,Earth and Space.
[7] De, Anirban (2012),Numerical simulation of surface explosions over dry, cohesionless soil., pp. 72–79, Journal of computer and geotechnics.
[8] Vasilis KARLOS , George SOLOMOS (2013),Calculation of Blast Loads for Application to Structural Components, European Commission.
[9] Ben Young, Ehab Ellobody (2006), Experimental investigation of concrete- filled cold-formed high strength stainless steel tube columns. Journal of Constructional Steel Research, 62 , pp. 484–492.
[10] XU, Guofu. and Deng, Zhengdong (2013), Analytic Solution of the Dynamic Response of Buried Pipelines under Indirect Ground Shock of Nuclear Blast, Journal of Engineering (JOE),Vol. 1, No. 3, pp. 49-52.
[11] Livemore Software Technology Corporation (LSTC).LS-DYNA Keyword User's manual, California, USA; 2003.
[12] Wu C., Oehlers D.J., Rebentrost M., Leach J., Whittaker A.S (2009),Blast testing of ultra-high performance fibre and FRP-retrofitted concrete slabs. Engineering Structures, 31(9): 2060-2069.
[13] Tham, C. Y (2006), Numerical and Empirical Approach In Predicting of a Concrete Target by an Ogive-Nosed Projectile, Int. J. Finite Element in Analysys and Dsign. 42, pp. 1258-1268.